REVISITING HIGHER-ORDER GRADIENT METHODS FOR MULTI-AGENT REINFORCEMENT LEARNING

Anonymous authors
Paper under double-blind review

ABSTRACT

This paper revisits Higher-Order Gradient (HOG) methods for Multi-Agent Reinforcement Learning (MARL). HOG methods are algorithms in which agents use higher-order gradient information to account for other agents' anticipated learning, and are shown to improve coordination in games with self-interested agents. So far, however, HOG methods are only applied to games with low-dimensional state spaces due to inefficient computation and preservation of higher-order gradient information. In this work, we solve these limitations and propose a HOG framework that can be applied to games with higher-dimensional state spaces. Moreover, we show that current HOG methods, when applied to games with common-interested agents, i.e., team games, can lead to miscoordination between the agents. To solve this, we propose Hierarchical Reasoning (HR) to improve coordination in team games, and we experimentally show that our proposed HR significantly outperforms state-of-the-art methods in standard multi-agent games. With our contributions, we greatly improve the applicability of HOG methods for MARL. For reproducibility, the code used for our work will be shared after the reviewing process.

1 INTRODUCTION

In multi-agent systems, the paradigm of *agents' reasoning about other agents* has been explored and researched extensively (Goodie et al., 2012; Stuhlmüller & Goodman, 2014; Liu & Lakemeyer, 2021). Recently, this paradigm is being studied in the subfield of Multi-Agent Reinforcement Learning (MARL) (Wen et al., 2019; 2020; Konan et al., 2022). Generally speaking, MARL deals with several agents simultaneously learning and interacting in an environment. In the context of MARL, reasoning can be interpreted as accounting for the anticipated learning of other agents (Zhang & Lesser, 2010; Willi et al., 2022). As MARL uses gradient-based optimization, learning anticipation naturally leads to the usage of higher-order gradient information (Foerster et al., 2018a; Letcher et al., 2019). The so-called Higher-Order Gradient (HOG) methods use this extra gradient information to predict and, in some cases, shape the learning of other agents (Letcher et al., 2019). The importance of prediction and shaping has been frequently shown for various games, such as the Iterated Prisoner's Dilemma (IPD), where shaping ensures cooperation between the agents (Foerster et al., 2018a). However, current HOG methods have clear limitations, as they can only work for specific types of games, and become inefficient when the dimensionality of the game increases. In this paper, we explore these limitations and propose a framework that can extend the application scope of HOG methods to a broader range of problem settings in MARL.

The vast majority of existing HOG methods focus only on games with low-dimensional state spaces, e.g., matrix games (Zhang & Lesser, 2010; Foerster et al., 2018a;c; Letcher et al., 2019; Willi et al., 2022). There are two challenges that limit HOG methods from being applied to games with high-dimensional state spaces: inefficient computation and preservation of higher-order gradient information. Specifically, current implementations of HOG methods require multiple data sampling stages to compute higher-order gradient information (Foerster et al., 2018c). Moreover, the higher-order gradient information is applied and, more importantly, preserved in the policy network's parameter space. As a result, existing HOG methods become very inefficient when applied to games that have high-dimensional state spaces, and therefore require high-dimensional parameter spaces. In this paper, to solve this, we propose an HOG framework where the higher-order gradient information are computed and preserved more efficiently. By comparing our proposed framework to existing HOG

methods in well-controlled studies, we demonstrate that the overall performance and efficiency of our proposed framework stay consistent with increased dimensionality, unlike for existing HOG methods, where they get drastically worse.

In addition to dimensionality limitations, the generalizability of HOG methods to various types of games is questionable. Originally, HOG methods are proposed to improve cooperation in games with self-interested agents (Zhang & Lesser, 2010; Foerster et al., 2018a). So far, however, it is unclear how HOG methods perform when agents are fully cooperative, i.e., for common-interested agents in team games. We demonstrate that existing HOG methods have the tendency to lead to miscoordination between common-interested agents, causing a sub-optimal overall reward. To solve this, and improve the applicability of HOG methods to team games, we propose Hierarchical Reasoning (HR), a new HOG methodology explicitly developed for improving coordination in games with common-interested agents. We compare our proposed methodology with state-of-the-art MARL algorithms, and show that we outperform existing methods on several fully-cooperative and mixed cooperative-competitive games.

2 Related works

When direct communication between agents is not possible, the standard tool for MARL agents to apply reasoning is Agents Modeling Agents (AMA) (Albrecht & Stone, 2018; Hernandez-Leal et al., 2019). Although agents traditionally use AMA to only predict the behavior of others (He et al., 2016; Hong et al., 2018), recent studies have extended AMA to further consider multiple levels of reasoning over the predicted behaviors (Wen et al., 2019; 2020). However, these approaches do not explicitly account for the other agents' anticipated learning, which has shown to be beneficial in games where interaction between self-interested agents naturally leads to worst-case outcomes (Zhang & Lesser, 2010; Foerster et al., 2018a).

HOG methods, on the other hand, are a range of methods that use higher-order gradient information to predict and, in some cases, shape the anticipated learning of other agents directly. This includes Learning with Opponent-Learning Awareness (LOLA), proposed to shape opponents for better coordination in Iterated Prisoner's Dilemma (IPD) by Foerster et al. (2018a), Look-Ahead (LA), proposed to guarantee convergence in cyclic games by Zhang & Lesser (2010), Stable Opponent Shaping (SOS), developed by Letcher et al. (2019) as an interpolation between LOLA and LA to inherit the benefits of both, and other methods such as Consensus Optimization (CO) and Symplectic Gradient Adjustment (SGA), that are proposed to improve cooperation by Bertsekas (2014) and Balduzzi et al. (2018), respectively. However, as we explain in Section 4, these methods have only been applied to simple games due to the challenges in computation and preservation of higher-order gradient information. Furthermore, the impact of current HOG methods on coordination between common-interested agents has not yet been fully investigated. Current investigations are limited to convergence and non-convergence to stable and unstable fixed points in differential games, respectively (Letcher et al., 2019). However, we demonstrate in Section 5.1 that in the case of a two-agent, two-action coordination game with unstable fixed points, HOG methods can converge to miscoordination points. The focus of this work is to extend current HOG methodology so that it can be used for games with higher-dimensional state spaces and common-interested agents.

3 Background

We formulate the MARL setup as a Markov Game (MG) (Littman, 1994). An MG is a tuple $(\mathcal{N}, \mathcal{S}, \{\mathcal{A}_i\}_{i\in\mathcal{N}}, \{\mathcal{R}_i\}_{i\in\mathcal{N}}, \mathcal{T}, \rho, \gamma)$, where $\mathcal{N}$ is the set of agents ($|\mathcal{N}| = n$), $\mathcal{S}$ is the set of states, and $\mathcal{A}_i$ is the set of possible actions for agent $i \in \mathcal{N}$. Agent i chooses its action $a_i \in \mathcal{A}_i$ through the policy network $\pi_{\theta_i} : \mathcal{S} \times \mathcal{A}_i \rightarrow [0, 1]$ parameterized by θ_i conditioning on the given state $s \in \mathcal{S}$. Given the actions of all agents, each agent i obtains a reward r_i according to its reward function $\mathcal{R}_i : \mathcal{S} \times \mathcal{A}_1 \times ... \times \mathcal{A}_n \rightarrow \mathbb{R}$. Given an initial state, the next state is produced according to the state transition function $\mathcal{T} : \mathcal{S} \times \mathcal{A}_1 \times ... \times \mathcal{A}_n \rightarrow \mathcal{S}$. We denote an episode of horizon T as $\tau = (\{s^0, a_1^0, ..., a_n^0, r_1^0, ..., r_n^0\}, ..., \{s^T, a_1^T, ..., a_n^T, r_1^T, ..., r_n^T\})$, and the discounted return for each agent i at time step $t \leq T$ is defined by $G_i^t(\tau) = \sum_{l=t}^{T} \gamma^{l-t} r_i$ where γ is a predefined discount factor. The expected return given the agents' policy parameters approximates the state value function for each agent $V_i(s, \theta_1, ..., \theta_n) = \mathbb{E}[G_i^t(\tau|s^t = s)]$. Each agent i aims to maximize the

expected return given the distribution of the initial state $\rho(s)$, denoted by the performance objective $J_i = \mathbb{E}_{\rho(s)} V_i(s, \theta_1, ..., \theta_n)$. A *naïve agent* updates its policy parameters in the direction of the objective's gradient: $\nabla_{\theta_i} J_i = \mathbb{E}_{\rho(s)} \nabla_{\theta_i} V_i(s, \theta_1, ..., \theta_n)$.

Learning With Opponent-Learning Awareness (LOLA). Unlike naïve agents, LOLA agents modify their learning objectives by differentiating through the anticipated learning steps of the opponents (Foerster et al., 2018a). Given $n = 2$ for simplicity, a first-order LOLA agent assumes a naïve opponent and optimizes $V_1^{\text{LOLA}}(s, \theta_1, \theta_2 + \Delta\theta_2)$ where $\Delta\theta_2 = \eta \nabla_{\theta_2} V_2(s, \theta_1, \theta_2)$ and η is the prediction length. Using first-order Taylor expansion, and by differentiating with respect to θ_1, the gradient adjustment for the first LOLA agent (Foerster et al., 2018a) is given by

$$\nabla_{\theta_1} V_1^{\text{LOLA}}(s, \theta_1, \theta_2 + \Delta\theta_2) \approx \nabla_{\theta_1} V_1 + (\nabla_{\theta_2 \theta_1} V_1)^{\intercal} \Delta\theta_2 + \underbrace{(\nabla_{\theta_1} \Delta\theta_2)^{\intercal} \nabla_{\theta_2} V_1}_{\text{shaping}}, \tag{1}$$

where $V_1 = V_1(s, \theta_1, \theta_2)$. The rightmost term in the LOLA update allows for active shaping of the opponent's learning. This term has been proven effective in enforcing cooperation in various games, including IPD (Foerster et al., 2018a;c). The LOLA update can be further extended to non-naïve opponents, resulting in higher-order LOLA agents (Foerster et al., 2018a; Willi et al., 2022).

Look Ahead (LA). LA agents assume that the opponents' learning steps cannot be influenced, i.e., cannot be shaped (Zhang & Lesser, 2010; Letcher et al., 2019). In other words, agent 1 assumes that the prediction step, $\Delta\theta_2$, is independent of the current optimization, i.e., $\nabla_{\theta_1} \Delta\theta_2 = 0$. Therefore, the shaping term disappears and the gradient adjustment for the first LA agent will be

$$\nabla_{\theta_1} V_1^{\text{LA}}(s, \theta_1, \theta_2 + \Delta\theta_2) \approx \nabla_{\theta_1} V_1 + (\nabla_{\theta_2 \theta_1} V_1)^{\intercal} \Delta\theta_2. \tag{2}$$

4 A HOG FRAMEWORK FOR HIGH-DIMENSIONAL STATE SPACES

Existing HOG methods like LOLA and LA are only applied to games with low-dimensional state spaces, e.g., matrix games (Zhang & Lesser, 2010; Foerster et al., 2018c;a; Letcher et al., 2019; Willi et al., 2022). When applied to games with higher-dimensional state spaces, they become very inefficient, due to the way the higher-order gradient information is computed and preserved. In this section, we analyze these problems, and we propose a framework that makes HOG practical for application to games with high-dimensional state spaces.

4.1 LIMITATIONS OF EXISTING HOG APPROACHES

Computation of higher-order gradient. Existing HOG methods are implemented in the stochastic policy gradient framework, and optimize non-differentiable objectives. Furthermore, the learning step for one agent in the standard stochastic policy gradient theorem is independent of other agents' parameters. Therefore, higher-order mixed partial derivatives (between multiple agents) cannot be easily computed. Foerster et al. (2018c) proposed an infinitely differentiable Monte Carlo estimator, referred to as DiCE, to correctly optimize the stochastic objectives with any order of gradients. Similarly to meta-learning frameworks, the agents reason about and predict the learning process of the opponents using inner learning loops and update their parameters in outer learning loops. However, each learning loop for each agent requires a sampling stage which is very inefficient for high-order reasoning and games with higher-dimensional state spaces, i.e., beyond matrix games.

Preservation of higher-order gradient information. HOG methods should constantly compute and update the higher-order gradient values and computation graphs that keep track of how the gradients should flow. In the implementation of existing HOG methods, the higher-order gradient information is computed and preserved in the parameter spaces of the agents' policy networks (Foerster et al., 2018a;c). As a result, the agents should either have access to other agents' exact parameters or infer other agents' parameters from state-action trajectories (Foerster et al., 2018a). In many game settings, these parameters are obscured. Moreover, when the dimensionality of state spaces increases, e.g., when having images as input, the dimensionality of the parameter spaces increases as well, making the parameter inference problem computationally expensive. Furthermore, computing and storing the higher-order gradient information in high-dimensional parameter spaces is inefficient, whether the parameters are inferred or exact.

4.2 HOG-MADDPG

To efficiently compute any-order mixed partial derivatives, we need to optimize differentiable objectives, which are directly dependent on all agents' parameters and can be efficiently estimated. The only platform that meets the above requirements and can deal with both discrete and continuous action spaces is Multi-Agent Deep Deterministic Policy Gradient (MADDPG) (Lowe et al., 2017). In this paradigm, decentralized policies are trained to optimize centralized, differentiable objectives, i.e., state-action value functions, that are estimated efficiently from trajectories sampled from a distinct behavior policy, i.e., the off-policy approach. This centralized training of decentralized policies is a standard paradigm for multi-agent planning (Kraemer & Banerjee, 2016; Foerster et al., 2018b; Peng et al., 2021). In this work, we aim to better exploit the opportunity for centralized learning by accounting for the agents' anticipated learning. Therefore, we propose to build our HOG framework on top of the MADDPG platform.

The only unsolved problem is the preservation of higher-order gradient information, as the centralized learning of MADDPG does not grant access to agents' parameters. To solve this, we propose to project the anticipated gradient information from the policies' parameter spaces to the action spaces. This way, 1) we avoid additional constraints above the centralized state-action value functions where the agents have access to all actions, and 2) we improve efficiency as the action spaces have significantly lower dimensionality than the policies' parameter spaces. In the following sections, we apply our proposed framework to two HOG methods and explain the details of their update rules for policy parameters. For all proposed methods in the HOG-MADDPG frameworks, the centralized state-action value functions are updated in a way identical to MADDPG (Lowe et al., 2017).

4.2.1 LA-MADDPG

In the MADDPG platform, a deterministic policy μ_{θ_i} for agent i is defined as $\mu_{\theta_i} : \mathcal{S} \rightarrow \mathcal{A}_i$, parameterized by θ_i. By denoting a centralized state-action function for each agent i as $Q_i(s, a_1, ..., a_n) = \mathbb{E}[G_i^t(\tau|s^t = s, a_i^t = a_i \forall i \in \mathcal{N})]$, the gradient of the MADDPG performance objective J_i with respect to θ_i can be approximated as:

$$\nabla_{\theta_i} J_i \approx \mathbb{E}_{\rho^\beta(s,\hat{a})} \nabla_{\theta_i} Q_i(s, \hat{a}_1, ..., a_i, ..., \hat{a}_n)|_{a_i=\mu_{\theta_i}(s)}, \tag{3}$$

where $\rho^\beta(s, \hat{a})$ is the state-action distribution of the behavior policy and $\hat{a} = \{\hat{a}_i \forall i \in \mathcal{N}\}$ are the actions sampled from the behavior policy during the exploration stage. Given $n = 2$ and a naïve opponent for simplicity, the gradient adjustment for parameters of the LA-MADDPG agent (θ_1) is computed by accounting for the anticipated policy parameters of the opponent, i.e., $\hat{\theta}_2 + \Delta\hat{\theta}_2(s)$:

$$\nabla_{\theta_1} J_1^{\text{LA}} \approx \mathbb{E}_{\rho^\beta(s)} \nabla_{\theta_1} Q_1(s, a_1, \tilde{a}_2)|_{a_1=\mu_{\theta_1}(s), \tilde{a}_2=\mu_{\hat{\theta}_2+\Delta\hat{\theta}_2}(s)}, \tag{4}$$

where $\Delta\hat{\theta}_2 = \eta \nabla_{\hat{\theta}_2} Q_2(s, \hat{a}_1, \hat{a}_2)|_{\hat{a}_1=\mu_{\hat{\theta}_1}(s), \hat{a}_2=\mu_{\hat{\theta}_2}(s)}$, and $\hat{\theta}_1$ and $\hat{\theta}_2$ are the behavior policy parameters. As the agents cannot have access to these parameters, we propose to project the anticipated gradient information to the action space (with the detailed derivation provided in Appendix A.1):

$$\nabla_{\theta_1} J_1^{\text{LA}} \approx \mathbb{E}_{\rho^\beta(s,\hat{a})} \nabla_{\theta_1} \mu_{\theta_1}(s) \nabla_{a_1} Q_1(s, a_1, \hat{a}_2 + \Delta\hat{a}_2)|_{a_1=\mu_{\theta_1}(s)}, \tag{5}$$

where $\Delta\hat{a}_2 = \hat{\eta} \nabla_{\hat{a}_2} Q(s, \hat{a}_1, \hat{a}_2)$ and $\hat{\eta}$ is the projected prediction length (see Alg. 1).

4.2.2 LOLA-MADDPG

In the standard MADDPG, it is assumed that the opponents' actions are fixed during the optimization steps for the agents. This assumption is problematic for LOLA agents that require shaping on the opponents' learning steps. To make these dependencies possible, we employ the Centralized Policy Gradient (CPG) (Peng et al., 2021) to derive the learning step of the LOLA agents. In CPG-MADDPG, the gradient update in Eq. (3) is modified to:

$$\nabla_{\theta_i} J_i \approx \mathbb{E}_{\rho^\beta(s)} \nabla_{\theta_i} Q_i(s, a_1, ..., a_n)|_{a_i=\mu_{\theta_i}(s)\ \forall i \in \mathcal{N}}. \tag{6}$$

Again, we propose to project the anticipated gradient information to the action space. Given $n = 2$, the first-order LOLA-MADDPG agent updates the policy parameters through (see Appendix A.2 for full derivation):

$$\nabla_{\theta_1} J_1^{\text{LOLA}} \approx \mathbb{E}_{\rho^\beta(s)} \nabla_{\theta_1} \mu_{\theta_1}(s) \nabla_{a_1} Q_1(s, a_1, a_2 + \Delta a_2)|_{a_1=\mu_{\theta_1}(s), a_1=\mu_{\theta_2}(s)}, \tag{7}$$

where $\Delta a_2 = \hat{\eta} \nabla_{a_2} Q(s, a_1, a_2)$, which, unlike for LA-MADDPG, is a function of a_1 (see Alg. 2).

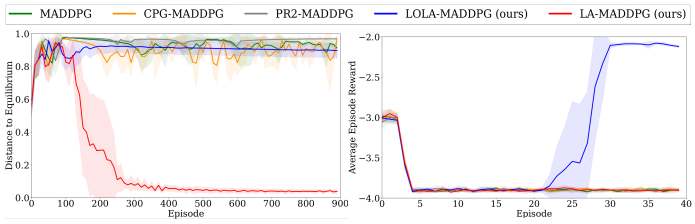

Figure 1: Learning curves in two matrix games. Left: Iterated Rotational Game in terms of the distance to the equilibrium point (↓). Right: Iterated Prisoner's Dilemma in terms of the normalized averages return (↑).

Method	IRG (DtE ↓)
LA-DiCE	0.09±0.07
LA-MADDPG (ours)	**0.03±0.02**

Method	IPD (AER ↑)
LOLA-DiCE	-2.16±0.12
LOLA-MADDPG (ours)	**-2.08±0.02**

Table 1: Comparisons of the LA and LOLA methods in the frameworks of DiCE and our proposed HOG-MADDPG.

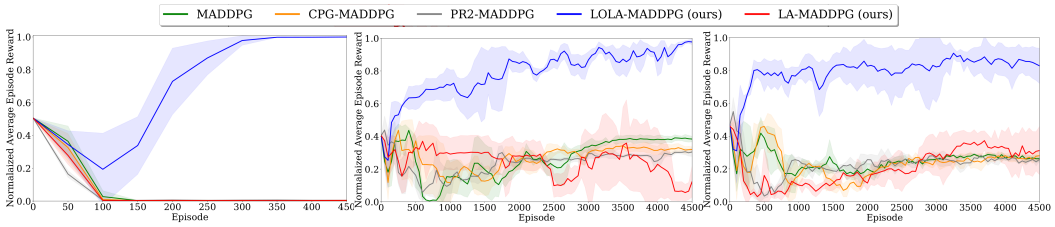

(a) Exit-Room level one. (b) Exit-Room level two. (c) Exit-Room level three.

Figure 2: Learning curves in different complexity levels of the exit-room game in terms of the normalized average return. Higher values are better.

4.3 Experiments

In this section, we first verify our proposed HOG-MADDPG methods on simple matrix games, to show how they work in the same situations as the original HOG methods. Second, we apply our proposed methods to games with high-dimensional state spaces, which is the envisioned use case for our methods, and evaluate the performance and efficiency. As the primary baselines, we apply HOG methods on the DiCE framework (Foerster et al., 2018c), i.e., LA-DiCE and LOLA-DiCE. We further compare our proposed methods with the standard MADDPG configured with three state-of-the-art update rules: 1) standard update rule (Lowe et al., 2017), referred to as MADDPG, 2) CPG update rule (Peng et al., 2021), referred to as CPG-MADDPG, and 3) Probabilistic Recursive Reasoning (PR2) update rule (Wen et al., 2019), referred to as PR2-MADDPG. For a fair comparison, we have employed identical architectures with the same number of policy and value function parameters for all the baseline (see Appendix C). Each experiment is repeated five times, and the results are reported in terms of mean and standard deviation. Unless mentioned otherwise, all the HOG methods are first-order.

4.3.1 Matrix Games

We evaluate the methods on the following commonly-used, two-agent matrix games: 1) Iterated Rotational Game (IRG) (Zhang & Lesser, 2010), a one-state game with a 1-Dimensional (1-D) continuous action space between 0 and 1 representing the probability of taking two discrete actions, and 2) Iterated Prisoner's Dilemma (IPD) (Foerster et al., 2018a), a five-state game with two discrete actions and $T = 150$. The games are developed to highlight the strengths of specific HOG methods (IRG for LA-based methods and IPD for LOLA). Further details about these games are provided in Appendix C.1. We evaluate the performances of methods based on the Distance to Equilibrium (DtE) in IRG (the equilibrium point in IRG is reached when $a_1 = a_2 = 0.5$) and the Averaged Episode Reward (AER) in IPD. In Figure 1, we depict the learning curves for our methods and other, state-of-the-art MADDPG-based algorithms. From this figure, we find that our HOG methods are the only MADDPG-based networks that can effectively solve these games, with LA-MADDPG for IRG and LOLA-MADDPG for IPD. This highlights the importance of using higher-order gradient information. To further show its effectiveness, we compare with current DiCE-based HOG methods (Foerster et al., 2018c) which are designed for these matrix games, in Table 1, and we find that we even achieve slightly better results.

	↑NAER in Exit-Room game			↓NTTI in Exit-Room game				
Methods	$l=1$	$l=2$	$l=3$	Naïve	1st-order	2nd-order	3rd-order	4th-order
LOLA-DiCE	0.91±0.04	0.68±0.06	0.56±0.12	1	2.39	3.74	5.12	6.41
LOLA-MADDPG (ours)	**1.00±0.00**	**0.99±0.01**	**0.93±0.03**	1	**1.03**	**1.05**	**1.08**	**1.12**

Table 2: Comparisons of DiCE with our proposed HOG-MADDPG in the Exit-Room game, in terms of performance (normalized average return in different game levels) and efficiency (training time per iteration in different reasoning levels).

4.3.2 MULTI-LEVEL EXIT-ROOM GAME

Inspired by Vinitsky et al. (2019), we propose an Exit-Room game with three levels of complexity (see Figure 3). The Exit-Room game is a grid-world variant of the IPD, with two agents (blue and red) and 15^{2l} states where $l \in \{1, 2, 3\}$ is the complexity level of the game. As in the standard IPD, the game is specifically developed to highlight the strength of LOLA. The agents should cooperate and move towards the exit doors on the right. However, they are tempted to exit the left doors, and in some cases, not exiting at all. In level 1, the agents have three possible actions (*move-left*, *move-right*, or *do nothing*), and in levels 2 and 3, they have additional *move-up* and *move-down* actions. Additionally, in level 3, the door positions are randomly located, resulting in more complex interactions between the agents. Each agent receives a 90×90 RGB image as the state observation. For more details about the game, see Appendix C.2.

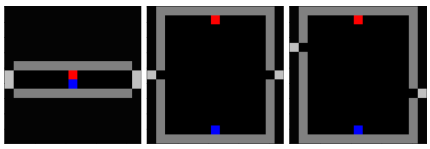

Figure 3: State observation in the Exit-Room game, level one (left), level two (middle), and level three (right).

Figure 2 compares the learning curves of LOLA-MADDPG with the state-of-the-art, MADDPG-based methods in terms of Normalized Average Episode Reward (NAER) which is the AER value that is normalized between the highest and lowest episode rewards in each game level. In Figure 2, we can clearly see that our LOLA-MADDPG significantly outperforms the other methods, similarly as for the matrix games. To highlight the benefits of our proposed method with respect to existing HOG methods, we compare our LOLA-MADDPG with LOLA-DiCE in terms of performance (by comparing NAER) and training efficiency, in Table 2. For training efficiency, we use the average Training Time per Iteration (TTI) for various opponents' reasoning levels. For a fair comparison, we report Normalized TTI (NTTI) for both methods, which are the normalized TTI values with respect to naïve (zero-order) version of each method. Observing Table 2, it is apparent that LOLA-DiCE fails to acquire the highest rewards, particularly for the second and third levels of the game, where complexity is increased. Moreover, our proposed LOLA-MADDPG performs better in all levels of the Exit-Room game in terms of NAER, and is also significantly more efficient in training, especially as the reasoning level of the opponent increases. This emphasizes the strength of our method, and shows that we have overcome the limitations of HOG methods described in Section 4.1.

5 A HOG METHODOLOGY FOR COMMON-INTERESTED AGENTS

Current HOG methods are proposed to enforce coordination in games with self-interested agents. In many applications, however, agents should cooperate to increase a common reward function, i.e., as a team game. As multiple agents should interact and cooperate, anticipating the learning of other agents, which is the core idea of HOG methods, has the potential to work well in these types of games too. In this section, we first show that standard HOG methods do not work well for team games, because they suffer from miscoordination. Subsequently, we propose a method to overcome this limitation, and evaluate it for several different games.

5.1 MISCOORDINATION ANALYSIS IN COOPERATIVE SCENARIOS

To investigate the effectiveness of HOG methods on the coordination between common-interested agents, we consider a two-agent, two-action coordination game (Claus & Boutilier, 1998) with an added miscoordination penalty. The game is defined by a common reward matrix $R = \left[\begin{smallmatrix} a & k \\ k & a \end{smallmatrix}\right]$, where $a > 0$ is coordination reward and $k \leq 0$ is the miscoordination penalty. We further define $g = a - k > 0$ as the miscoordination regret. The agents are parameterized by $\theta_1 \in [0, 1]$ and

$\theta_2 \in [0, 1]$, denoting the probability of choosing the first action by agent one and two, respectively. Similarly to Singh et al. (2000); Zhang & Lesser (2010), we analyze the dynamics of θ_1 and θ_2 for LOLA, LA, and naïve agents to investigate the coordination behaviors.

Theorem 1 *If, in the previously defined two-person, two-action coordination game with a miscoordination regret g, the agents are updated following the LA method and a fixed prediction length η, then they are subject to miscoordination for $g > \frac{1}{2\eta}$. If the agents are updated following the LOLA method and a fixed prediction length η, then they are subject to miscoordination for $g > \frac{1}{4\eta}$. If the agents follow the naïve updates, then they are never subject to miscoordination for any value of g.*
Proof – See Appendix B.1.

A closer inspection of the HOG methods reveals two important aspects about their fundamental ideas. First, anticipating other agents' learning is only effective when it is close to their true future learning. Existing HOG methods assume a reasoning level for other agents. If this assumption is wrong, it can negatively affect the coordination between the cooperative agents. Second, the idea of shaping other agents' learning can be misleading if the other agents do not follow, making agents more likely to suffer from miscoordination. We hypothesize that by addressing these two aspects of current HOG methods, miscoordination between agents can be avoided.

5.2 Hierarchical Reasoning

Based on our hypothesis, we propose *Hierarchical Reasoning* (HR), an HOG methodology especially designed for cooperative agents. In contrast to standard HOG methods, HR determines a hierarchy among the agents in each training iteration, which determines the reasoning orders of the agents. Concretely, if $n = 2$, and we assume that the first agent is the *leader* and the second agent is the *follower*, the gradient adjustment for the leader is similar to first-order LOLA agents, and is given by

$$\nabla_{\theta_1} V^{\text{Leader}}(s, \theta_1, \theta_2 + \Delta\theta_2) \approx \nabla_{\theta_1} V + (\nabla_{\theta_2\theta_1} V)^\intercal \Delta\theta_2 + (\nabla_{\theta_1} \Delta\theta_2)^\intercal \nabla_{\theta_2} V, \tag{8}$$

where $V = V(s, \theta_1, \theta_2)$ is the common value function, and $\Delta\theta_2 = \eta \nabla_{\theta_2} V$. However, unlike LOLA agents, the leader knows the reasoning level of the follower, which is a naïve agent. The plan for the leader is to change its parameters $\bar{\theta}_1 = \theta_1 + \nabla_{\theta_1} V^{\text{Leader}}(s, \theta_1, \theta_2 + \Delta\theta_2)$ in such a way that an optimal increase in the common value is achieved, after its new parameters are taken into account by the follower. Therefore, the follower must follow the plan and adjust its parameters through

$$\nabla_{\theta_2} V^{\text{Follower}}(s, \bar{\theta}_1, \theta_2) \approx \nabla_{\theta_2} V + (\nabla_{\theta_1\theta_2} V)^\intercal \nabla_{\theta_1} V^{\text{Leader}}(s, \theta_1, \theta_2 + \Delta\theta_2), \tag{9}$$

Theorem 2 *If, in the previously defined two-person, two-action coordination game with a miscoordination regret g, the agents are updated following the HR methodology, then they are not subject to miscoordination for any value of g.*
Proof – See Appendix B.2.

With this, we have shown that HR naturally avoids miscoordination and therefore, our hypothesis is correct. However, the main goal is to demonstrate that HR improves coordination between common-interested agents with respect to naïve learning, which does not take into account higher-order gradients at all. If HR does not improve the coordination, there is no clear benefit over the naïve learners, as they also avoid miscoordination. To show the benefits of HR, we employ a standard two-agent, three-action coordination game (Claus & Boutilier, 1998). The game has a common reward matrix $R = \left[\begin{smallmatrix} 10 & 0 & k \\ 0 & 2 & 0 \\ k & 0 & 10 \end{smallmatrix}\right]$, and we define $g = 10 - k$ as the miscoordination regret. Each agent is parameterized with three parameters: θ^1, θ^2, and θ^3 ($\theta^i > 0 \ \forall i \in \{1, 2, 3\}$ and $\sum_i^3 \theta^i = 1$), representing the probability of taking the actions a^1, a^2, and a^3, respectively. The game has two global equilibrium points (if $\theta^1 = 1$ or $\theta^3 = 1$ for all agents), and one local equilibrium point (if $\theta^2 = 1$ for all agents). In Figure 4, we depict the converged results for this game for naïve, LA, LOLA, and HR agents, for various values of miscoordination regret g. The experiments are run 500 times until

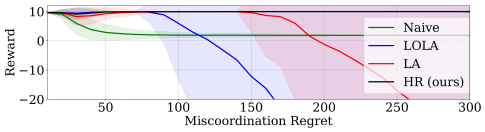

Figure 4: Converged results for various values of miscoordination regret.

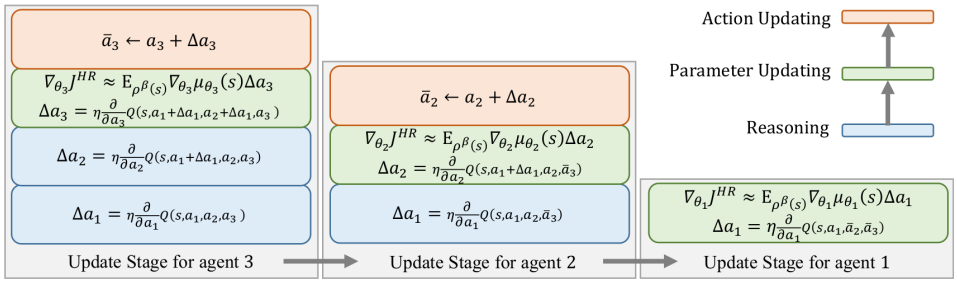

Figure 5: An example of the parameter update stages in HR-MADDPG, for a game with three common-interested agents $m = 3$, assigned to three hierarchy levels.

convergence, with random initializations. From 4, we find that both LA and LOLA agents are subject to miscoordination for high values of g, which is consistent with our findings for the two-action coordination game. However, the most interesting aspect of this experiment is that by increasing the value of g, the coordination between the naïve agents reduces, leading them to the local equilibrium point, whereas our HR agents consistently achieve the highest reward, independently of the miscoordination regret. This shows the benefit of HR agents over naïve agents.

5.2.1 HR-MADDPG

In this section, we propose HR-MADDPG, an extension of HOG-MADDPG for games with common-interested agents and high-dimensional state spaces. We first define $\mathcal{M} \subseteq \mathcal{N}$, as a set of common-interested agents such that $R_i = R_j \ \forall i, j \in \mathcal{M}$. Without the loss of generality, we consider $\mathcal{M} = \mathcal{N}$, i.e., team games with a common state-action value function $Q(s, a_1, ..., a_m)$.

Hierarchy level assignment. In the policy update step of HR-MADDPG, each agent is first assigned to one of $m = |\mathcal{M}|$ levels of hierarchy based on the amount of influence that it has on other agents, i.e., its shaping capacity, in each training iteration. The shaping capacity of the ith agent, f_i, is the sum of l^2-norms of the shaping term in Eq. 1 with respect to all other agents j:

$$f_i = \sum_{j \neq i \ \& \ \in \mathcal{M}} \left\| (\nabla_{a_i} \Delta a_j)^\intercal \nabla_{a_j} Q(a_1, ..., a_m) \right\|, \tag{10}$$

where $\Delta a_j = \nabla_{a_j} Q(a_1, ..., a_m)$. In each hierarchy level, the assigned agent is a leader of the lower hierarchy levels and a follower of the higher ones, with two reasoning rules: 1) a leader knows the reasoning levels of the followers and is one level higher, and 2) a follower cannot reason about the leaders and only follows their shaping plans. As HR-MADDPG benefits from centralized learning, the only constraint for these reasoning rules remains the centralized state-action value function.

Parameter update. After the hierarchy level assignment, the agents update their policy parameters in m update stages, i.e., one for each agent, and in a top-down fashion: the agent in the highest hierarchy level updates its policy parameters first. In each update stage, the corresponding agent 1) reasons about the followers (if any) in a bottom-up fashion, i.e., it reasons about the agent in the lowest hierarchy level first, 2) updates its policy parameters, and 3) updates its action for the next update stage (if any). Figure 5 demonstrates an example with the update stages for three common-interested agents 1, 2 and 3, that are assigned to hierarchy levels h^1, h^2, h^3, where agent 3, assigned to h^3 is the leader, etc. For the general cases of m agents, we provide the HR-MADDPG algorithm in Appendix A.3 (see Alg. 3).

5.3 Experiments

In this section, we aim to demonstrate the advantages of our proposed HR-MADDPG for games with common-interested agents, compared to 1) LA-MADDPG and LOLA-MADDPG, and 2) state-of-the-art methods: MADDPG (Lowe et al., 2017), CPG-MADDPG (Peng et al., 2021), and PR2-MADDPG (Wen et al., 2019). For this purpose, we first develop the Particle Coordination game to assess the coordination capability of the methods carefully. Then, we compare the general performance of all the methods in standard multi-agent games (Lowe et al., 2017; Peng et al., 2021). See Appendix C.3 and C.4 for details on the experiments.

5.3.1 Particle Coordination Game

Methods	↑NAER in Particle Environment			↑NAER in Mujoco Environment		
	Cooperative Navigation	Physical Deception	Predator-Prey	Half-Cheetah	Walker	Reacher
DDPG (LB)	0.00	0.00	0.00	0.00	0.00	0.00
C-MADDPG (UB)	1.00	1.00	1.00	1.00	1.00	1.00
MADDPG	0.77	0.61	0.21	0.86	0.45	0.02
CPG-MADDPG	0.78	0.67	0.18	0.88	0.46	0.05
PR2-MADDPG	0.78	0.54	0.08	0.85	0.45	0.01
LA-MADDPG	0.78	0.63	0.13	0.85	0.43	0.04
LOLA-MADDPG	0.77	0.56	0.13	0.83	0.42	0.01
HR-MADDPG (ours)	**0.88**	**0.83**	**0.44**	**0.94**	**0.67**	**0.42**

Table 3: Comparisons of methods in terms of the Normalized Average Episode Reward (NAER) for common-interested agents. LB: Lower Bound. UB: Upper Bound.

Our proposed game is a variant of the Cooperative Navigation game (Lowe et al., 2017) with two agents and three landmarks. The agents should select and approach one of the landmarks, and the landmark closest to an agent is considered to be the selected landmark. If the agents select and approach the same landmark, they receive global or local optimal rewards based on the selected landmark. They will receive an assigned miscoordination penalty if they select and approach different landmarks. In Figure 6, we depict the learning curves for our method and other MADDPG-based algorithms. From this figure, it is clear that our HR-MADDPG is the only method that consistently converges to the global optimum of the game, which is consistent with our previous results for the two-agent, three-action coordination game. Further experiments regarding the sensitivity of HOG-MADDPG methods to the prediction length are provided in Appendix C.3.

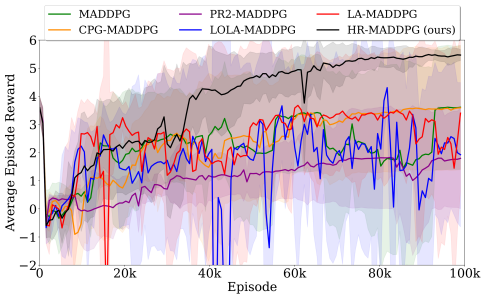

Figure 6: Learning curves in the Particle Coordination game. Higher values are better.

5.3.2 Standard multi-agent games

We evaluate the methods in three Particle environment games (Lowe et al., 2017): 1) Cooperative Navigation with three common-interested agents, 2) Physical Deception with two common-interested and one self-interested agent, and 3) Predator-Prey with two common-interested (predator) and one self-interested (prey) agents. Furthermore, we compare the methods in three games within the multi-agent Mujoco environment (Peng et al., 2021): 1) two-agent Half-Cheetah, 2) two-agent Walker, and 3) two-agent Reacher. In the mixed environments (Physical Deception and Predator-Prey), we have employed the MADDPG method for the self-interested agents. We report the Normalized Average Episode Reward for the common-interested agents in Table 3, where the normalization is done between the single-agent variant of MADDPG (DDPG (Lillicrap et al., 2016)) and a fully centralized (in learning and execution) variant of MADDPG, referred to as C-MADDPG. In Table 3, we observe that our proposed HOG-MADDPG consistently and significantly outperforms all the state-of-the-art MADDPG-based methods. Again, these results confirm that our proposed HR-MADDPG improves coordination between common-interested agents, leading to better results.

6 Discussion

In this paper, we proposed the HOG-MADDPG framework to make HOG methods applicable to games with high-dimensional state spaces. As a result, the benefits of HOG can now be used in many more MARL problems. As a first case study, we investigated the applicability of current HOG methodologies to team games, and found that they suffer from miscoordination, which we then solved with our proposed HR methodology. Like this solution, there are numerous other possibilities for extending HOG-MADDPG, e.g., restricting the centralized learning framework to the most relevant agents, which is essential in many-agent games. With our work, we aim to spark such new ideas for HOG methods in MARL, and we provide the framework to realize them.

REFERENCES

Stefano V Albrecht and Peter Stone. Autonomous agents modelling other agents: A comprehensive survey and open problems. *Artificial Intelligence*, 258:66–95, 2018.

David Balduzzi, Sebastien Racaniere, James Martens, Jakob Foerster, Karl Tuyls, and Thore Graepel. The mechanics of n-player differentiable games. In *International Conference on Machine Learning*, pp. 354–363. PMLR, 2018.

Dimitri P Bertsekas. *Constrained optimization and Lagrange multiplier methods*. Academic press, 2014.

Caroline Claus and Craig Boutilier. The dynamics of reinforcement learning in cooperative multiagent systems. *AAAI/IAAI*, 1998(746-752):2, 1998.

Thomas Degris, Martha White, and Richard Sutton. Off-Policy Actor-Critic. In *International Conference on Machine Learning*, 2012.

Stefan Elfwing, Eiji Uchibe, and Kenji Doya. Sigmoid-weighted linear units for neural network function approximation in reinforcement learning. *Neural Networks*, 107:3–11, 2018.

Jakob Foerster, Richard Y Chen, Maruan Al-Shedivat, Shimon Whiteson, Pieter Abbeel, and Igor Mordatch. Learning with Opponent-Learning Awareness. In *Proceedings of the 17th International Conference on Autonomous Agents and MultiAgent Systems*, pp. 122–130, 2018a.

Jakob Foerster, Gregory Farquhar, Triantafyllos Afouras, Nantas Nardelli, and Shimon Whiteson. Counterfactual multi-agent policy gradients. In *Proceedings of the AAAI Conference on Artificial Intelligence*, volume 32, 2018b.

Jakob Foerster, Gregory Farquhar, Maruan Al-Shedivat, Tim Rocktäschel, Eric Xing, and Shimon Whiteson. Dice: The infinitely differentiable monte carlo estimator. In *International Conference on Machine Learning*, pp. 1529–1538. PMLR, 2018c.

Adam S Goodie, Prashant Doshi, and Diana L Young. Levels of theory-of-mind reasoning in competitive games. *Journal of Behavioral Decision Making*, 25(1):95–108, 2012.

He He, Jordan Boyd-Graber, Kevin Kwok, and Hal Daumé III. Opponent modeling in deep reinforcement learning. In *International conference on machine learning*, pp. 1804–1813. PMLR, 2016.

Pablo Hernandez-Leal, Bilal Kartal, and Matthew E Taylor. A survey and critique of multiagent deep reinforcement learning. *Autonomous Agents and Multi-Agent Systems*, 33(6):750–797, 2019.

Zhang-Wei Hong, Shih-Yang Su, Tzu-Yun Shann, Yi-Hsiang Chang, and Chun-Yi Lee. A Deep Policy Inference Q-Network for Multi-Agent Systems. In *Proceedings of the 17th International Conference on Autonomous Agents and MultiAgent Systems*, pp. 1388–1396, 2018.

Eric Jang, Shixiang Gu, and Ben Poole. Categorical Reparametrization with Gumble-Softmax. In *International Conference on Learning Representations (ICLR 2017)*. OpenReview. net, 2017.

Diederik P Kingma and Jimmy Ba. Adam: A method for stochastic optimization. In *ICLR*, 2015.

Sachin Konan, Esmaeil Seraj, and Matthew Gombolay. Iterated Reasoning with Mutual Information in Cooperative and Byzantine Decentralized Teaming. *arXiv preprint arXiv:2201.08484*, 2022.

Landon Kraemer and Bikramjit Banerjee. Multi-agent reinforcement learning as a rehearsal for decentralized planning. *Neurocomputing*, 190:82–94, 2016.

Alistair Letcher, Jakob Foerster, David Balduzzi, Tim Rocktäschel, and Shimon Whiteson. Stable Opponent Shaping in Differentiable Games. In *International Conference on Learning Representations*, 2019.

Timothy P Lillicrap, Jonathan J Hunt, Alexander Pritzel, Nicolas Heess, Tom Erez, Yuval Tassa, David Silver, and Daan Wierstra. Continuous control with deep reinforcement learning. In *ICLR (Poster)*, 2016.

Michael L Littman. Markov games as a framework for multi-agent reinforcement learning. In *Machine learning proceedings 1994*, pp. 157–163. Elsevier, 1994.

Daxin Liu and Gerhard Lakemeyer. Reasoning about Beliefs and Meta-Beliefs by Regression in an Expressive Probabilistic Action Logic. In *international joint conference on artificial intelligence*. IJCAI, 2021.

Ryan Lowe, Yi Wu, Aviv Tamar, Jean Harb, Pieter Abbeel, and Igor Mordatch. Multi-agent actor-critic for mixed cooperative-competitive environments. *arXiv preprint arXiv:1706.02275*, 2017.

Bei Peng, Tabish Rashid, Christian Schroeder de Witt, Pierre-Alexandre Kamienny, Philip Torr, Wendelin Boehmer, and Shimon Whiteson. FACMAC: Factored Multi-Agent Centralised Policy Gradients. *NeurIPS*, 2021.

Satinder P Singh, Michael J Kearns, and Yishay Mansour. Nash Convergence of Gradient Dynamics in General-Sum Games. In *UAI*, pp. 541–548, 2000.

Andreas Stuhlmüller and Noah D Goodman. Reasoning about reasoning by nested conditioning: Modeling theory of mind with probabilistic programs. *Cognitive Systems Research*, 28:80–99, 2014.

Eugene Vinitsky, Natasha Jaques, Joel Leibo, Antonio Castenada, and Edward Hughes. An open source implementation of sequential social dilemma games. `https://github.com/eugenevinitsky/sequential_social_dilemma_games/issues/182`, 2019. GitHub repository.

Ying Wen, Yaodong Yang, Rui Luo, Jun Wang, and Wei Pan. Probabilistic recursive reasoning for multi-agent reinforcement learning. In *7th International Conference on Learning Representations, ICLR 2019*, 2019.

Ying Wen, Yaodong Yang, and Jun Wang. Modelling Bounded Rationality in Multi-Agent Interactions by Generalized Recursive Reasoning. In *IJCAI*, 2020.

Timon Willi, Alistair Hp Letcher, Johannes Treutlein, and Jakob Foerster. COLA: consistent learning with opponent-learning awareness. In *International Conference on Machine Learning*, pp. 23804–23831. PMLR, 2022.

Chongjie Zhang and Victor Lesser. Multi-agent learning with policy prediction. In *Proceedings of the AAAI Conference on Artificial Intelligence*, volume 24, 2010.

APPENDIX

A MORE DETAILS ON THE HOG-MADDPG METHODS

A.1 LA-MADDPG

In the standard MADDPG, the performance objective is defined as:

$$J_i = \mathbb{E}_{\rho^\beta(s,\hat{a})} Q_i(s, \hat{a}_1, ..., a_i, ..., \hat{a}_n, \theta_1, ..., \theta_n)|_{a_i=\mu_{\theta_i}(s)}, \tag{11}$$

where $\rho^\beta(s, \hat{a})$ is the state-action distribution of the behavior policy with $\hat{a} = \{\hat{a}_i \forall i \in \mathcal{N}\}$. The gradient of J_i with respect to θ_i can be approximated as:

$$\nabla_{\theta_i} J_i \approx \mathbb{E}_{\rho^\beta(s,\hat{a})} \nabla_{\theta_i} Q_i(s, \hat{a}_1, ..., a_i, ..., \hat{a}_n)|_{a_i=\mu_{\theta_i}(s)}, \tag{12}$$

where the direct dependencies of state-action value function to policy parameters can be dropped based on the proofs presented in Degris et al. (2012). Given $n = 2$ and a naïve opponent for simplicity, the gradient adjustment for parameters of the LA-MADDPG agent (θ_1) is computed by accounting for the anticipated policy parameters of the opponent, i.e., $\hat{\theta}_2 + \Delta\hat{\theta}_2(s)$:

$$\nabla_{\theta_1} J_1^{\text{LA}} \approx \mathbb{E}_{\rho^\beta(s)} \nabla_{\theta_1} Q_1(s, a_1, \tilde{a}_2)|_{a_1=\mu_{\theta_1}(s), \tilde{a}_2=\mu_{\hat{\theta}_2+\Delta\hat{\theta}_2}(s)}, \tag{13}$$

Algorithm 1: LA-MADDPG for a set of n self-interested agents ($\mathcal{N}$).

Initialize μ_{θ_i}, Q_i, μ'_i, and Q'_i $\forall i \in \mathcal{N}$
for episode $= 1$ to max-num-episodes **do**
  Receive initial state s
  for $t = 1$ to max-episode-length **do**
    Select action a_i from $\mu_{\theta_i}(s)$ and the exploration strategy $\forall i \in \mathcal{N}$
    Execute actions $a = \{a_i\}_{\forall i \in \mathcal{N}}$ and observe rewards $r = \{r_i\}_{\forall i \in \mathcal{N}}$ and new state s'
    Store the tuple (s, a, r, s') in replay buffer $\mathcal{D}$
    Set $s = s'$

    Sample a random K tuples $\{(s^k, a^k, r^k, s'^k)\}_{k \in \{1,...,K\}}$ from $\mathcal{D}$
    for agent $i = 1$ to n **do**
      Set $y_i^k = r_i^k + \gamma Q'_i(s'^k, a'_1, ..., a'_n)|_{a'_h = \mu'_h(s'^k)}$, for $k \in \{1, ..., K\}$
      Update state-action value function Q_i by minimizing:

$$\mathcal{L} = \frac{1}{K} \sum_{k \in \{1,...,K\}} [(Q_i(s^k, a_1^k, ..., a_m^k) - y_i^k)^2]$$

    end for
    for agent $i = 1$ to n **do**
      for agent $j = 1$ to n **do**
        if $j = i$ **then** continue
        Set $\Delta a_j^k = \eta \frac{\partial}{\partial a_j^k} Q_j(s^k, a_1^k, ..., a_m^k)$ for $k \in \{1, ..., K\}$
      end for
      Update policy parameters θ_i via: $\nabla_{\theta_i} J_i^{\text{LA}} \approx$

$$\frac{1}{K} \sum_{k \in \{1,...,K\}} \nabla_{\theta_i} \mu_{\theta_i}(s^k) \frac{\partial}{\partial a_i^k} Q_i(s^k, a_1^k + \Delta a_1^k, ..., a_i^k, ..., a_m^k + \Delta a_m^k)|_{a_i^k = \mu_{\theta_i}(s^k)}$$

    end for
    Update Q'_i and μ'_i $\forall i \in \mathcal{N}$
  end for
end for

where $\Delta\hat{\theta}_2 = \eta \nabla_{\hat{\theta}_2} Q_2(s, \hat{a}_1, \hat{a}_2)|_{\hat{a}_1 = \mu_{\hat{\theta}_1}(s), \hat{a}_2 = \mu_{\hat{\theta}_2}(s)}$, and $\hat{\theta}_1$ and $\hat{\theta}_2$ are the behavior policy parameters. As the agents cannot have access to these parameters, we propose to project the anticipated gradient information to the action space using first-order Taylor expansion:

$$\begin{aligned} \tilde{a}_2 &= \mu_{\hat{\theta}_2 + \Delta\hat{\theta}_2}(s) \\ &\approx \mu_{\hat{\theta}_2}(s) + (\Delta\hat{\theta}_2)^\intercal \nabla_{\hat{\theta}_2} \mu_{\hat{\theta}_2}(s) \end{aligned} \tag{14}$$

Given that:

$$\begin{aligned} \Delta\hat{\theta}_2 &= \eta \nabla_{\hat{\theta}_2} Q_2(s, \hat{a}_1, \hat{a}_2) \\ &= \eta \nabla_{\hat{\theta}_2} \mu_{\hat{\theta}_2}(s) \left(\nabla_{\hat{a}_2} Q_2(s, \hat{a}_1, \hat{a}_2)|_{\hat{a}_2 = \mu_{\hat{\theta}_2}(s)} \right)^\intercal, \end{aligned} \tag{15}$$

we have:

$$\begin{aligned} \tilde{a}_2 &\approx \mu_{\hat{\theta}_2}(s) + \left(\eta \nabla_{\hat{\theta}_2} \mu_{\hat{\theta}_2}(s) \left(\nabla_{\hat{a}_2} Q_2(s, \hat{a}_1, \hat{a}_2) \right)^\intercal \right)^\intercal \nabla_{\hat{\theta}_2} \mu_{\hat{\theta}_2}(s) \\ &= \mu_{\hat{\theta}_2}(s) + \nabla_{\hat{a}_2} Q_2(s, \hat{a}_1, \hat{a}_2) \left(\eta \nabla_{\hat{\theta}_2} \mu_{\hat{\theta}_2}(s) \right)^\intercal \nabla_{\hat{\theta}_2} \mu_{\hat{\theta}_2}(s) \\ &= \mu_{\hat{\theta}_2}(s) + \nabla_{\hat{a}_2} Q_2(s, \hat{a}_1, \hat{a}_2) \eta \left\| \nabla_{\hat{\theta}_2} \mu_{\hat{\theta}_2(s)} \right\|^2 \\ &= \mu_{\hat{\theta}_2}(s) + \nabla_{\hat{a}_2} Q_2(s, \hat{a}_1, \hat{a}_2) \hat{\eta}, \end{aligned} \tag{16}$$

Algorithm 2: LOLA-MADDPG for a set of n self-interested agents ($\mathcal{N}$).

Initialize μ_{θ_i}, Q_i, μ'_i, and Q'_i $\forall i \in \mathcal{N}$
for episode $= 1$ to max-num-episodes **do**
  Receive initial state s
  for $t = 1$ to max-episode-length **do**
    Select action a_i from $\mu_{\theta_i}(s)$ and the exploration strategy $\forall i \in \mathcal{N}$
    Execute actions $a = \{a_i\}_{\forall i \in \mathcal{N}}$ and observe rewards $r = \{r_i\}_{\forall i \in \mathcal{N}}$ and new state s'
    Store the tuple (s, a, r, s') in replay buffer $\mathcal{D}$
    Set $s = s'$

    Sample a random K tuples $\{(s^k, a^k, r^k, s'^k)\}_{k \in \{1,...,K\}}$ from $\mathcal{D}$
    for agent $i = 1$ to n **do**
      Set $y_i^k = r_i^k + \gamma Q'_i(s'^k, a'_1, ..., a'_n)|_{a'_h = \mu'_h(s'^k)}$, for $k \in \{1, ..., K\}$
      Update state-action value function Q_i by minimizing:

$$\mathcal{L} = \frac{1}{K} \sum_{k \in \{1,...,K\}} [(Q_i(s^k, a_1^k, ..., a_m^k) - y_i^k)^2]$$

    end for
    Set $a_i^k = \mu_{\theta_i}(s^k)$, for $k \in \{1, ..., K\}$ and $i \in \mathcal{N}$
    for agent $i = 1$ to n **do**
      for agent $j = 1$ to n **do**
        if $j = i$ **then** continue
        Set $\Delta a_j^k = \eta \frac{\partial}{\partial a_j^k} Q_j(s^k, a_1^k, ..., a_m^k)$ for $k \in \{1, ..., K\}$
      end for
      Update policy parameters θ_i via: $\nabla_{\theta_i} J_i^{\text{LA}} \approx$

$$\frac{1}{K} \sum_{k \in \{1,...,K\}} \nabla_{\theta_i} \mu_{\theta_i}(s^k) \frac{\partial}{\partial a_i^k} Q_i(s^k, a_1^k + \Delta a_1^k, ..., a_i^k, ..., a_m^k + \Delta a_m^k)$$

    end for
    Update Q'_i and μ'_i $\forall i \in \mathcal{N}$
  end for
end for

where $\|.\|$ is the l^2-norm and we have defined the projected prediction length $\hat{\eta} = \eta \left\| \nabla_{\hat{\theta}_2} \mu_{\hat{\theta}_2(s)} \right\|^2$ since $\left\| \nabla_{\hat{\theta}_2} \mu_{\hat{\theta}_2(s)} \right\|^2$ is a positive number and independent of θ_1. Therefore:

$$\begin{aligned} \tilde{a}_2 &\approx \mu_{\hat{\theta}_2}(s) + \hat{\eta} \nabla_{\hat{a}_2} Q_2(s, \hat{a}_1, \hat{a}_2) \\ &= \hat{a}_2 + \Delta \hat{a}_2. \end{aligned} \tag{17}$$

Replacing Eq. 17 in Eq. 13 yields Eq. 5:

$$\nabla_{\theta_1} J_1^{\text{LA}} \approx \mathbb{E}_{\rho^\beta(s, \hat{a})} \nabla_{\theta_1} \mu_{\theta_1}(s) \nabla_{a_1} Q_1(s, a_1, \hat{a}_2 + \Delta \hat{a}_2)|_{a_1 = \mu_{\theta_1}(s)}. \tag{18}$$

For the general cases of n agents, refer to Alg. 1.

A.2 LOLA-MADDPG

In CPG-MADDPG, the gradient update is:

$$\nabla_{\theta_i} J_i \approx \mathbb{E}_{\rho^\beta(s)} \nabla_{\theta_i} Q_i(s, a_1, ..., a_n)|_{a_i = \mu_{\theta_i}(s) \ \forall i \in \mathcal{N}}. \tag{19}$$

Given $n = 2$ and a naïve opponent for simplicity, the gradient adjustment for parameters of the LOLA-MADDPG agent (θ_1) is computed by accounting for the anticipated policy parameters of the opponent, i.e., $\theta_2 + \Delta\theta_2(s)$:

$$\nabla_{\theta_1} J_1^{\text{LOLA}} \approx \mathbb{E}_{\rho^\beta(s)} \nabla_{\theta_1} Q_1(s, a_1, \tilde{a}_2)|_{a_1 = \mu_{\theta_1}(s), \tilde{a}_2 = \mu_{\theta_2 + \Delta\theta_2}(s)}, \tag{20}$$

Algorithm 3: HR-MADDPG for a set of m common-interested agents ($\mathcal{M}$).

Initialize μ_{θ_i}, Q_i, μ'_i, and Q'_i $\forall i \in \mathcal{N}$
for episode $= 1$ to max-num-episodes **do**
  Receive initial state s
  for $t = 1$ to max-episode-length **do**
    Select action a_i from $\mu_{\theta_i}(s)$ and the exploration strategy $\forall i \in \mathcal{M}$
    Execute actions $a = \{a_i\}_{\forall i \in \mathcal{M}}$ and observe common reward r and new state s'
    Store the tuple (s, a, r, s') in replay buffer $\mathcal{D}$
    Set $s = s'$

    Sample a random K tuples $\{(s^k, a^k, r^k, s'^k)\}_{k \in \{1,...,K\}}$ from $\mathcal{D}$
    Set $y^k = r^k + \gamma Q'(s'^k, a'_1, ..., a'_m)|_{a'_h = \mu'_h(s'^k)}$, for $k \in \{1, ..., K\}$
    Update state-action value function Q by minimizing:

$$\mathcal{L} = \frac{1}{K} \sum_{k \in \{1,...,K\}} [(Q(s^k, a^k_1, ..., a^k_m) - y^k)^2]$$

    Assign the agents into m hierarchy levels using Eq. 10
    Set $a^k_i = \mu_{\theta_i}(s^k)$, for $k \in \{1, ..., K\}$ and $i \in \mathcal{M}$
    for agent $i = m$ to 1 **do**
      for agent $j = 1$ to i **do**
        Compute Δa^k_j, for $k \in \{1, ..., K\}$:
        if $j = 1$ & $i \neq m$ **then** $\Delta a^k_1 = \eta \frac{\partial}{\partial a^k_1} Q(s^k, a^k_1, ..., a^k_i, \bar{a}^k_{i+1}, ..., \bar{a}^k_m)$
        elif $j \neq 1$ & $i = m$ **then** $\Delta a^k_j = \eta \frac{\partial}{\partial a^k_j} Q(s^k, a^k_1 + \Delta a^k_1, ..., a^k_{j-1} + \Delta a^k_{j-1}, a^k_j, ..., a^k_m)$
        elif $j = 1$ & $i = m$ **then** $\Delta a^k_1 = \eta \frac{\partial}{\partial a^k_1} Q(s^k, a^k_1, ..., a^k_m)$
        else $\Delta a^k_j = \eta \frac{\partial}{\partial a^k_j} Q(s^k, a^k_1 + \Delta a^k_1, ..., a^k_{j-1} + \Delta a^k_{j-1}, a^k_j, \bar{a}^k_{j+1}, ...\bar{a}^k_m)$
      end for
      Update policy parameters θ_i via:

$$\nabla_{\theta_i} J^{\text{HR}}_i \approx \frac{1}{K} \sum_{k \in \{1,...,K\}} \nabla_{\theta_i} \mu_{\theta_1}(s^k) \Delta a^k_i$$

      Set $\bar{a}^k_i = \text{detach}(a^k_i + \Delta a^k_i)$, for $k \in \{1, ..., K\}$
    end for
    Update Q'_i and μ'_i $\forall i \in \mathcal{M}$
  end for
end for

where $\Delta\theta_2 = \eta \nabla_{\theta_2} Q_2(s, a_1, a_2)|_{a_1 = \mu_{\theta_1}(s), a_2 = \mu_{\theta_2}(s)}$, and unlike for LA-MADDPG, is a function of θ_1. Again, we propose to project the anticipated gradient information to the action space. Given that:

$$\Delta\theta_2 = \eta \nabla_{\theta_2} \mu_{\theta_2}(s) \left(\nabla_{a_2} Q_2(s, a_1, a_2)|_{a_1 = \mu_{\theta_1}(s), a_2 = \mu_{\theta_2}(s)} \right)^{\intercal}, \tag{21}$$

we have:

$$\begin{aligned} \tilde{a}_2 &= \mu_{\theta_2 + \Delta\theta_2}(s) \\ &\approx \mu_{\theta_2}(s) + (\Delta\theta_2)^{\intercal} \nabla_{\theta_2} \mu_{\theta_2}(s) \\ &= \mu_{\theta_2}(s) + \nabla_{a_2} Q_2(s, a_1, a_2) \eta \left\| \nabla_{\theta_2} \mu_{\theta_2(s)} \right\|^2 \\ &= \mu_{\theta_2}(s) + \nabla_{a_2} Q_2(s, a_1, a_2) \hat{\eta}, \end{aligned} \tag{22}$$

where $\|.\|$ is the l^2-norm and we have defined the projected prediction length $\hat{\eta} = \eta \left\| \nabla_{\theta_2} \mu_{\theta_2(s)} \right\|^2$ since $\left\| \nabla_{\theta_2} \mu_{\theta_2(s)} \right\|^2$ is a positive number and independent of θ_1. Therefore:

$$\tilde{a}_2 \approx a_2 + \Delta a_2. \tag{23}$$

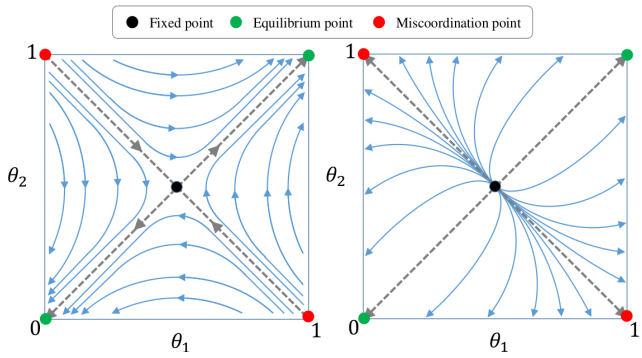

Figure 7: Phase planes of the LA and LOLA dynamics. Left: unstable fixed point. Right: unstable saddle fixed point.

Replacing Eq. 23 in Eq. 20 yields Eq. 7:

$$\nabla_{\theta_1} J_1^{\text{LOLA}} \approx \mathbb{E}_{\rho^\beta(s)} \nabla_{\theta_1} \mu_{\theta_1}(s) \nabla_{a_1} Q_1(s, a_1, a_2 + \Delta a_2)|_{a_1=\mu_{\theta_1}(s), a_1=\mu_{\theta_2}(s)}. \tag{24}$$

For the general cases of n agents, refer to Alg. 2.

A.3 HR-MADDPG

For the general cases of m agents, we provide the HR-MADDPG algorithm in Alg. 3.

B More details on the miscoordination analyses

The two-agent, two-action coordination game (Claus & Boutilier, 1998) is defined by a common reward matrix $R = \left[\begin{smallmatrix} a & k \\ k & a \end{smallmatrix}\right]$, where $a > 0$ is coordination reward and $k \leq 0$ is the miscoordination penalty. We further define $g = a - k > 0$ as the miscoordination regret. Let $\theta_1 \in [0, 1]$ and $\theta_2 \in [0, 1]$ denote the probability of choosing the first action by first and second agents, respectively. The common value function $V(\theta_1, \theta_2) = 2g(\theta_1\theta_2) - g(\theta_1 + \theta_2) + a$ is the expected reward, given θ_1 and θ_2. The game has two equivalent Nash equilibria: $\theta_1 = \theta_2 = 0$ and $\theta_1 = \theta_2 = 1$. We further define two miscoordination points: $(\theta_1 = 1, \theta_2 = 0)$ and $(\theta_1 = 0, \theta_2 = 1)$.

B.1 Proof of Theorem 1

Given Eq. 2 the unconstrained dynamics of LA agents can be defined by the following differential equations :

$$\begin{bmatrix} \partial\theta_1/\partial t \\ \partial\theta_2/\partial t \end{bmatrix} = \begin{bmatrix} 4\eta g^2 & 2g \\ 2g & 4\eta g^2 \end{bmatrix} \begin{bmatrix} \theta_1 \\ \theta_2 \end{bmatrix} - \begin{bmatrix} 2\eta g^2 + g \\ 2\eta g^2 + g \end{bmatrix} \tag{25}$$

This system of equations has a unique fixed point (zero gradients) at $\theta_1 = \theta_2 = 0.5$ (see Figure 7). The eigenvalue analysis of the coefficient matrix yields two real eigenvalues, $\lambda_1 = 4\eta g^2 + 2g$ and $\lambda_2 = 4\eta g^2 - 2g$, and two respective diagonal and off-diagonal eigenvectors. While λ_1 is always positive, the sign of λ_2 depends on the values of both η and g. For a fixed prediction length, non-positive values of λ_2 are reached by $g \leq \frac{1}{2\eta}$. In this case, the fixed point is an unstable saddle point (or unstable line in case of $\lambda_2 = 0$), and the agents, with any initial values of θ_1 and θ_2 (except on the fixed point itself), converge to the equilibrium points (see Figure 7-Left). However, when the miscoordination regret increases, $g > \frac{1}{2\eta}$, the fixed point becomes an unstable (source) point (see Figure 7-Right). Therefore, some initial values of θ_1 and θ_2 naturally lead to the miscoordination points.

In the case of LoLA agents, the unconstrained dynamics can be defined as:

$$\begin{bmatrix} \partial\theta_1/\partial t \\ \partial\theta_2/\partial t \end{bmatrix} = \begin{bmatrix} 8\eta g^2 & 2g \\ 2g & 8\eta g^2 \end{bmatrix} \begin{bmatrix} \theta_1 \\ \theta_2 \end{bmatrix} - \begin{bmatrix} 4\eta g^2 + g \\ 4\eta g^2 + g \end{bmatrix} \tag{26}$$

This system of equations has a unique fixed point, again at $\theta_1 = \theta_2 = 0.5$ (see Figure 7). The eigenvalue analysis of the coefficient matrix yields two real eigenvalues, $\lambda_1 = 8\eta g^2 + 2g$ and

$\lambda_2 = 8\eta g^2 - 2g$, and two respective diagonal and off-diagonal eigenvectors. Similar to the case of LA agents, λ_1 is always positive and the sign of λ_2 depends on the values of both η and g. For a fixed prediction length, non-positive values of λ_2 are reached by $g \leq \frac{1}{4\eta}$. In this case, the fixed point is an unstable saddle point (or unstable line in case of $\lambda_2 = 0$), and the agents, with any initial values of θ_1 and θ_2 (except on the fixed point itself), converge to the equilibrium points. However, when the miscoordination regret increases, $g > \frac{1}{4\eta}$, the fixed point becomes an unstable (source) point. Therefore, some initial values of θ_1 and θ_2 naturally lead to the miscoordination points.

In the case of the naïve agents, we have:

$$\begin{bmatrix} \partial\theta_1/\partial t \\ \partial\theta_2/\partial t \end{bmatrix} = \begin{bmatrix} 0 & 2g \\ 2g & 0 \end{bmatrix} \begin{bmatrix} \theta_1 \\ \theta_2 \end{bmatrix} - \begin{bmatrix} g \\ g \end{bmatrix} \tag{27}$$

Similar to the case of LOLA and LA, this system of equations has a unique fixed point (zero gradients) at $\theta_1 = \theta_2 = 0.5$. The eigenvalue analysis of the coefficient matrix yields two real eigenvalues, $\lambda_1 = 2g$ and $\lambda_2 = -2g$, and two respective diagonal and off-diagonal eigenvectors. This time, however, the eigenvalues are of opposite signs for any values of g and the fixed point is always an unstable saddle point. Therefore, any initial values of θ_1 and θ_2 (except on the fixed point itself) naturally lead to the equilibrium points.

Based on these results, we hypothesize that 1) wrong reasoning level assumptions and 2) shaping plans that are not followed can lead to miscoordination points. Both LOLA and LA agents assume that other agents are naïve learners, which is obviously a wrong assumption since all agents conduct first-order reasoning. For self-interested agents, it is natural for the agents to don't unveil their reasoning order to each other. as they have different goals. However, common-interested agents can benefit more from this reasoning information to achieve their common goal. Furthermore, LOLA agents constantly underestimate other LOLA agents and try to shape them. This is while other LOLA agents do not follow the plan, and each tries to show that it is smarter than the others. Letcher et al. (2019) shows that these arrogant behaviors lead to outcomes that are strictly worse for everyone. It is also clear from Theorem 1 that the range of g that leads to miscoordination in LOLA ($g > \frac{1}{4\eta}$) is larger than the range of g in LA ($g > \frac{1}{2\eta}$).

In the above coordination game, one general solution to reduce the possibility of miscoordination is decreasing the prediction length's values. However, in non-tabular settings, with large state spaces, it is infeasible to estimate the miscoordination regret and adjust the prediction length accordingly. Furthermore, the prediction length directly affects the usage of higher-order gradient information, and further reducing the prediction length ($\eta \to 0$) leads to the naïve learners.

B.2 Proof of Theorem 2

Given Eqs. 9 and 8, the unconstrained dynamics of the HR agents can be defined by the following differential equations :

$$\begin{bmatrix} \partial\theta_1/\partial t \\ \partial\theta_2/\partial t \end{bmatrix} = \begin{bmatrix} 8\eta g^2 & 2g \\ 2g + 16\eta^2 g^3 & 4\eta g^2 \end{bmatrix} \begin{bmatrix} \theta_1 \\ \theta_2 \end{bmatrix} - \begin{bmatrix} 4\eta g^2 + g \\ 8\eta^2 g^3 + 4\eta g^2 + g \end{bmatrix} \tag{28}$$

resulting in a unique fixed point at $\theta_1 = \theta_2 = 0.5$ and two real eigenvalues, $\lambda = 6\eta g^2 \pm 2p\sqrt{9eta^2 g^2 + 1}$. Unlike the case of LOLA and LA, the eigenvalues are now of opposite signs for any values of g, and the fixed point is always an unstable saddle point. Therefore, any initial values of θ_1 and θ_2 (except on the fixed point itself) naturally lead to the equilibrium points.

C More details on the experiments and the implementations

In this section, we describe all the experiments and the implementations in detail. To ease the reproducibility of our work, the code of our methods and experiments are shared with the community at [`to comply with the double-blind policy, the link will be inserted in the final version`].

A note on partial observability. So far, we have formulated the MARL setup as an MG, where it is assumed that the agents have access to the state space. However, in many games, the agents only receive a private state observation of the current state. In this case, the MARL setup can be

	discrete action 1	discrete action 2
discrete action 1	$(0, 3)$	$(3, 2)$
discrete action 2	$(1, 0)$	$(2, 1)$

Table 4: Reward matrix in IRG.

	Cooperate	Defect
Cooperate	$(-1, -1)$	$(-3, 0)$
Defect	$(0, -3)$	$(-3, -3)$

Table 5: Reward matrix in IPD.

formulated as a Partially Observable Markov Game (PO-MG) (Littman, 1994). A PO-MG is a tuple $(\mathcal{N}, \mathcal{S}, \{\mathcal{A}_i\}_{i\in\mathcal{N}}, \{\mathcal{O}_i\}_{i\in\mathcal{N}}, \{\mathcal{R}_i\}_{i\in\mathcal{N}}, \mathcal{T}, \{\Omega_i\}_{i\in\mathcal{N}}, \rho, \gamma)$, where $\mathcal{O}_i$ is the set of sate observations for agent $i \in \mathcal{N}$. Each agent i chooses its action $a_i \in \mathcal{A}_i$ through the policy $\pi_{\theta_i} : \mathcal{O}_i \times \mathcal{A}_i \to [0, 1]$ parameterized by θ_i conditioning on the given state observation $o_i \in \mathcal{O}_i$. After transition to a new state, each agent i receives a private state observation through its observation function $\Omega_i : \mathcal{S} \to \mathcal{O}_i$. In this case, the centralized state-action value function for each agent i is defined as $Q_i(o_1, ..., o_n, a_1, ..., a_n) = \mathbb{E}[G_i^t(\tau|s^t = s, o_i = \Omega_i(s) \ \& \ a_i^t = a_i \forall i \in \mathcal{N})]$. Therefore, the proposed HOG-MADDPG framework can be modified accordingly.

C.1 Matrix games

Iterated Rotational Game (IRG)(Zhang & Lesser, 2010) is a one-state, two-agent, one-action matrix game with the reward matrices depicted in Table 4 (for two discrete actions). Each agent must choose a 1-D continuous action (a_1 for agent one and a_2 for agent two) representing the probability of taking two discrete actions. The game has a unique equilibrium point at $a_1 = a_2 = 0.5$, which is also the fixed point of the game. IRG is originally proposed to demonstrate the circular behavior that can emerge if the agents follow the naïve gradient updates. LA agents, on the other hand, can quickly converge to the equilibrium point by considering their opponent's parameter adjustment. As LOLA agents cannot preserve the fixed point of the game (Letcher et al., 2019), they converge to non-equilibrium points. We evaluate the performances of methods based on the Distance to Equilibrium (DtE).

Iterated Prisoner's Dilemma (IPD) (Foerster et al., 2018a) is a five-state, two-agent, two-action game with the reward matrices depicted in Table 5. Each agent must choose between two discrete actions (cooperate or defect). The game is played for 150 time steps ($T = 150$). In the one-shot version of the game, there is only one Nash equilibrium for the agents (Defect, Defect). In the iterated games, (Defect, Defect) is also a Nash equilibrium. However, a better equilibrium is Tit-For-Tat (TFT), where the players start by cooperating and then repeat the previous action of the opponents. The LOLA agents can shape the opponent's learning to encourage cooperation and, therefore, converge to TFT (Letcher et al., 2019). We evaluate the methods' performances based on the Averaged Episode Reward (AER).

Implementation details. We used policies and state-action value functions with the same neural network architecture in all methods. We employed Multi-Layer Perceptron (MLP) networks with two hidden layers of dimension 64 for policies and state-action value functions. In order to make the value functions any-order differentiable, we used SiLU nonlinear function (Elfwing et al., 2018) in between the hidden layers. For IRG, we used the Sigmoid function in the policies to output 1-D continues action, and for IPD, we used the Gumble-softmax function (Jang et al., 2017) in the policies to output two discrete actions. The algorithms are trained for 900 (in IRG) and 50 (in IPD) episodes by running Adam optimizer (Kingma & Ba, 2015) with a fixed learning rate of 0.01. The prediction length, η, for LOLA and LA agents in both HOG-MADDPG and DiCE frameworks are fixed to 1 in all experiments. We reported the best methods' performances in Table 1. All experiments are repeated five times, and the results are reported in terms of mean and standard deviation in Figure 1 and Table 1.

C.2 Exit-Room game

The Exit-Room game is a grid-world variant of the IPD, with two agents (blue and red) and 15^{2l} states where $l \in \{1, 2, 3\}$ is the complexity level of the game. The agents should cooperate and move towards the exit doors on the right. However, they are tempted to exit the left doors and, in some cases, not exiting at all. In level 1, the agents have three possible actions (*move-left*, *move-right*, or

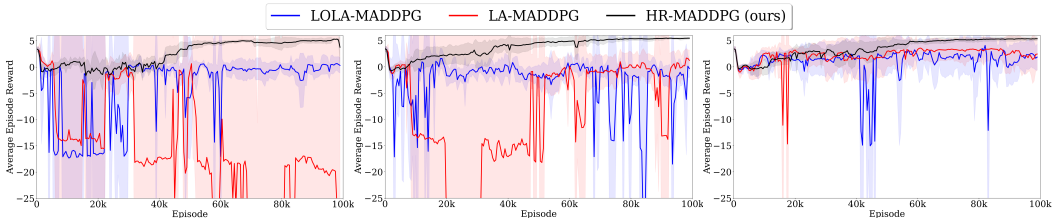

(a) $\eta = 1$ (b) $\eta = 0.1$ (c) $\eta = 0.01$

Figure 8: Learning curves in the particle coordination game with different values of the prediction length, η, for HOG-MADDPG methods.

do nothing), and the reward is computed as Vinitsky et al. (2019):

$$\begin{aligned} \text{reward}_C &= \lambda_C(\text{cooperation}_{self} + \text{cooperation}_{opponent}) \\ \text{reward}_D &= \lambda_D(1 - \text{cooperation}_{self}) \\ \text{reward} &= \text{reward}_C + \text{reward}_D, \end{aligned} \tag{29}$$

where λ_C and λ_D are some constants, and $\text{cooperation}_{self}$ and $\text{cooperation}_{opponent}$ are the normalized distances of the agent and its opponent to the right door, respectively. In levels 2 and 3, the agents have additional *move-up* and *move-down* actions. In level 3, the door positions are randomly located, resulting in more complex interactions between the agents. In addition to the reward in Eq. (29), the agents receive an additional reward for approaching the doors in levels 2 and 3. Each agent receives four 90×90 RGB images representing the state observations of the last four time steps.

Implementation details. As before, we used policies and state-action value functions with the same neural network architecture in all methods. Both policy and value networks consist of two parts: encoder and decoder. The encoders are CNN networks with three convolutional layers ($12 \times 90 \times 90 \rightarrow 32 \times 21 \times 21 \rightarrow 64 \times 9 \times 9 \rightarrow 64 \times 7 \times 7$) and two fully connected layers ($3136 \rightarrow 512 \rightarrow 128$), with SiLU nonlinear functions (Elfwing et al., 2018) in between. The decoders are MLP networks with two hidden layers of dimension 64 for policies and state-action value functions. We used the Gumble-softmax function in the policies (Jang et al., 2017) to output the discrete actions. The algorithms are trained for 450 (in level one) and 4500 (in levels two and three) episodes by running Adam optimizer (Kingma & Ba, 2015) with a fixed learning rate of 0.01. The prediction length, η, for LOLA and LA agents in both HOG-MADDPG and DiCE frameworks are fixed to 1 in all experiments. All experiments are repeated five times, and the results are reported in terms of mean and standard deviation in Figure 2 and Table 2. The methods are evaluated in terms of the Normalized Average Episode Reward (NAER), where the normalization is done between the highest and lowest episode rewards in each game level. We reported the best methods' performances in Table 2.

C.3 Particle Coordination Game

Our proposed game is a variant of the Cooperative Navigation game in the Particle environment (Lowe et al., 2017). As shown in Figure 9, each one of the two agents (purple circles) should select and approach one of the three landmarks (one gray and two green circles). Landmarks are selected based on the closest distance between the agent and the landmarks. Suppose the agents select and approach the same landmark. In that case, they receive global (by selecting the green landmarks) or local (by selecting the gray landmark) optimal rewards. They will receive an assigned miscoordination penalty if they select and approach different landmarks. Each agents receive a 14-D state observation vector and select a 5-D, one-hot vector, representing one of the five discrete actions: *move-right*, *move-left*, *move-up*, *move-down*, and *stay*. The horizon is set to 25, $T = 25$. The agents receive a Landmark Selection (LS) reward indicated by the

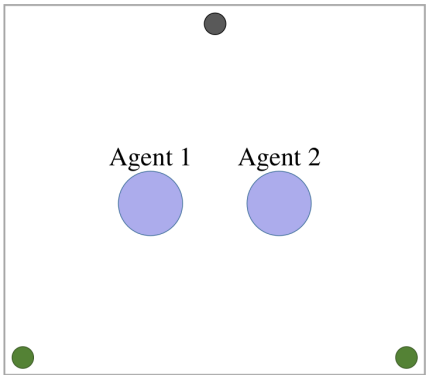

Figure 9: Particle coordination game with two agents and three landmarks.

	Particle Environment			Mujoco Environment		
	Cooperative Navigation	Physical Deception	Predator-Prey	Half-Cheetah	Walker	Reacher
Observation	18-D	10-D (8-D)	14-D (12-D)	11-D	11-D	8-D
Action	5-D	5-D (5-D)	5-D (5-D)	3-D	3-D	1-D
Action type	discrete	discrete	discrete	continuous	continuous	continuous
Horizon (step)	25	25	25	100	300	50

Table 6: Specifications in the standard multi-agent games. In the mixed environments, the dimensions are reported as "d_1 (d_2)" where d_1 is the dimension for common-interested agents and d_2 is the dimension for self-interested ones.

matrix: $R_{\text{LS}} = \begin{bmatrix} 2 & 0 & -20 \\ 0 & 0.4 & 0 \\ -20 & 0 & 2 \end{bmatrix}$, where the rows and columns indicate the selected landmarks by the first and second agents, respectively. Furthermore, the agents receive an additional reward for approaching the landmarks.

Implementation details. We used policies and state-action value functions with the same neural network architecture in all methods. We employed MLP networks with two hidden layers of dimension 64 for policies and state-action value functions with SiLU nonlinear functions (Elfwing et al., 2018) in between. We used the Gumble-softmax function (Jang et al., 2017) in the policies to output the discrete actions. The algorithms are trained for 100k episodes by running Adam optimizer (Kingma & Ba, 2015) with a fixed learning rate of 0.01. We set the prediction length, η, to 0.1 for HR agents and 0.01 for LOLA and LA agents. All experiments are repeated five times, and the results are reported in terms of mean and standard deviation in Figure 6.

Effect of the prediction length. Additionally, we illustrate the effect of various prediction lengths on the performance of HR, LOLA, and LA agents in Figure 8. As shown, the HR-MADDPG method consistently converges to the global optimum of the game. This is while both LOLA-MADDPG and LA-MADDPG demonstrate weak performances, especially by increasing the prediction length.

C.4 STANDARD MULTI-AGENT GAMES

We evaluate the methods in three Particle environment games (Lowe et al., 2017): 1) Cooperative Navigation with three common-interested agents, 2) Physical Deception with two common-interested and one self-interested agent, and 3) Predator-Prey with two common-interested (predator) and one self-interested (prey) agents. Furthermore, we compare the methods in three games within the multi-agent Mujoco environment (Peng et al., 2021): 1) two-agent Half-Cheetah, 2) two-agent Walker, and 3) two-agent Reacher. In the mixed environments (Physical Deception and Predator-Prey), we have employed the MADDPG method for the self-interested agents. Games' specifications are reported in Table 6. We created separate validation and test sets for each game that included 100 and 300 randomly generated scenarios, respectively. In each game, we save the models that have the best performance on the validation set and test them on the test set to report the results. All experiments are repeated five times, and the mean results are reported in Table 3 in terms of the Normalized Average Episode Reward (NAER). The normalization is done between the single-agent variant of MADDPG (DDPG (Lillicrap et al., 2016)) and a fully centralized (in learning and execution) variant of MADDPG, referred to as C-MADDPG. The non-normalized data are reported in Table 8 in terms of the Collective Average Episode Reward (CAER) for the common-interested agents.

Implementation details. As before, we used policies and state-action value functions with the same neural network architecture in all methods. We employed MLP networks with two hidden layers (of dimension 64 for the Particle environment and 256 for the Mujoco environment) for policies and state-action value functions with SiLU nonlinear functions (Elfwing et al., 2018). In the Particle environment, We used the Gumble-softmax function (Jang et al., 2017) in the policies to output the discrete actions and trained the algorithms for 100k episodes by running Adam optimizer (Kingma & Ba, 2015) with a fixed learning rate of 0.01. In the Mujoco environment, we used the Tanh function in the policies to output the continuous actions and train the algorithms for 10k episodes by running Adam optimizer (Kingma & Ba, 2015) with a fixed learning rate of 0.001. The prediction lengths, η, in HR-MADDPG, LA-MADDPG, and LOLA-MADDPG are optimized between $0.001 - 0.1$ in all games. We avoid considering any smaller value than 0.001 for the prediction length as it makes

	η in Particle Environment			η in Mujoco Environment		
	Cooperative Navigation	Physical Deception	Predator-Prey	Half-Cheetah	Walker	Reacher
LA-MADDPG	0.002	0.003	0.01	0.001	0.002	0.003
LOLA-MADDPG	0.001	0.003	0.008	0.001	0.001	0.002
HR-MADDPG	0.003	0.01	0.04	0.004	0.004	0.007

Table 7: The optimized prediction lengths for HOG-MADDPG methods.

the algorithms similar to the naïve learners. The optimized prediction lengths are reported in Table 7.

Ablation study. We have additionally conducted an ablation study on the hierarchy level assignments in the HR-MADDPG. Rather than iteratively sorting the agents based on their shaping capacities through Eq. (10), we randomly assigned the agents to hierarchy levels in the beginning and fixed the hierarchy levels throughout the optimization. This variant of the HR-MADDPG, referred to as HR-MADDPG (F), is evaluated and compared in Table 9. As can be seen, using the proposed sorting strategy based on the shaping capacities of the agents, as done in our HR-MADDPG, constantly improves performance.

	↑CAER in Particle Environment			↑CAER in Mujoco Environment		
Methods	Cooperative Navigation	Physical Deception	Predator-Prey	Half-Cheetah	Walker	Reacher
DDPG (LB)	-189.18	13.04	10.20	611.74	2925.17	-16.19
C-MADDPG (UB)	-130.91	20.82	20.87	1564.60	6362.36	-8.89
MADDPG	-144.02	17.82	12.46	1435.93	4482.31	-16.02
CPG-MADDPG	-143.96	18.29	12.08	1454.62	4511.08	-15.84
PR2-MADDPG	-143.67	17.26	11.08	1418.69	4473.14	-16.09
LA-MADDPG	-143.72	17.92	11.58	1424.39	4408.56	-15.89
LOLA-MADDPG	-144.21	17.43	11.54	1406.61	4369.13	-16.13
HR-MADDPG	**-137.63**	**19.48**	**14.85**	**1503.07**	**5226.26**	**-13.16**

Table 8: Comparisons of methods in terms of the Collective Average Episode Reward (CAER) for common-interested agents, corresponding to the normalized data in Table 3.

	↑NAER in Particle Environment			↑NAER in Mujoco Environment		
Methods	Cooperative Navigation	Physical Deception	Predator-Prey	Half-Cheetah	Walker	Reacher
HR-MADDPG (F)	0.85	0.80	0.38	0.92	0.63	0.38
HR-MADDPG	**0.88**	**0.83**	**0.44**	**0.94**	**0.67**	**0.42**

Table 9: Ablation study on the hierarchy level assignments in our HR-MADDPG method.